

## Synthesis of Mesoporous Silicate Molecular Sieves

RAHMATOLLAH RAHIMI\*, M. Anbia, G.H. MOHAMNEZHAD and M. RABAN  
*Department of Chemistry, Iran University of Science and Technology, Tehran, Iran*  
*Fax: (98)(21)77491204; E-mail: rahimi\_rah@iust.ac.ir*

In this studies, surfactant hegzadesil 3-methyl ammonium chloride was used as a structural informant or mould for synthesis of mesoporous silicate molecular sieves. Many of the mesoporous titanium silicates were synthesized by adding titanium compounds to the mixture, but considerable ratio of titanium centers placed in the frame are not accessible. This disadvantage was compensated by titanium butoxide as a titanous compound after being linked to the interior surfaces of host mesoporous. The mesoporous silicate was synthesized by, S<sup>+</sup>I method and then titanium was linked into the cavities. The structure of synthesized compound was characterized and studied by using XRD, XRF, TGA, SEM, IR techniques and surface adsorption of nitrogen. The results showed the formation of meso structure with hexagonal cavities, high surface area, isomorphic cavities, spherical morphology, functional groups and the amount of titanium input into the structure.

**Key Words: Surfactant hegzadesil, Mesoporous silicate, 3-Methyl ammonium chloride, XRD, XRF, TGA, SEM, Techniques.**

### INTRODUCTION

Nowadays, many attentions have been attracted toward the selective oxidation by solid catalyses<sup>1</sup>. Until the end of 70th decade, ion exchange was the main method for metals coordination to microporous matrix, which creates big difficulty for metal separation in liquid phase oxidation<sup>2</sup>. A break in which titanium embedded into the silicate structure was obtained by exploring titanium silicate (TS-1)<sup>3,4</sup>. Based on these information many titano silicate microporous such as TS-2<sup>5</sup>, Ti-ZSM-48<sup>6</sup>, Ti-β<sup>7</sup> and titanium aluminum phosphate, TAPO-5<sup>8</sup>, TAPO-36<sup>9</sup> and TAPO-34<sup>10</sup> were provided. The general problem of these materials is the small size of their cavities that limits accessibility of important and large substrates.

Exploring the M41S family<sup>11</sup>, created a new path for preparing the titanosilicates and provided the possibility for selective oxidation of larger substrates. Many of mesoporous titanium silicates including Ti-MCM-41<sup>12,13</sup>, Ti-HMS<sup>13,14</sup>, Ti-MCM-48<sup>15</sup> and silaned Ti-MCM-41<sup>16</sup> were prepared by adding titanous compounds to synthesized mixture. But a considerable number of titanium centers placed in its frame are inaccessible. When interior surfaces of host mesoporous are linked to synthesized titanium catalysis precursor, this weak point can be compensated. So, the applied method for synthesis of titanium mesoporous silicate in this project is based on

linkage after synthesis. It means that at first, mesoporous material is synthesized and then titanous compounds are linked in its cavities.

In this article, the structure is characterized and studied after the synthesis process of titanium mesoporous silicate completed. The presented methods included X-ray diffraction measurements at low angles, infrared spectrometry, superficial absorption of nitrogen for studying superficial area, cavity volume, distribution of cavity sizes on the basis of BET, BJH and SEM methods, elemental analysis and XRF.

## EXPERIMENTAL

**Synthesis of mesoporous silicate:** According to performed tests, we need a certain ratio of surfactant to silica to obtain considered structure. Mole ratio of surfactant to silica was 0.5 and surfactant quantity was 0.05 molar. To provide silicate solution, at first 40 g distilled water was added in balloon placed on stirrer and then 20.5 g sodium silicate added. Then 1.2 g of sulphuric acids was added to this solution and stirred for 10 min. Surfactant solution was provided by combining 31.15 g surfactant with 40.5 g distilled water. After 10 min, surfactant solution was added to silicate solution. The obtained gel was stirred for 0.5 h, then 20 g of water added to it and refluxed for 144 h in 100 °C. After setting, it had been cold to ambient temperature, the sediment filtered and washed with double distilled water and placed in ambient temperature to dry overnight. The obtained white solid material divided into two parts. In order to extract the compound from mould, one part transferred into porcelain cup and placed into furnace. As observed in Fig. 1, furnace heat was increased from ambient temperature to 550 °C with 3 °C/min temperature slant. Then it remained in this temperature for 7 h. The temperature decreased to ambient temperature with former slant.

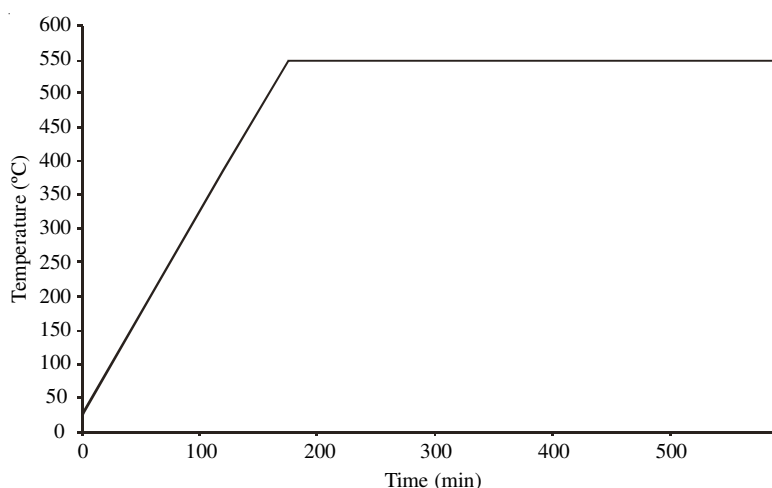


Fig. 1. Curve of furnace temperature program for calcinations

**Synthesis of titanium mesoporous silicate:** In pervious step, calcinated material set in autoclave at 40 °C for 2 h for removing superficial observed waters. Then certain amount of sample weighed and transferred into balloon. About 25 mL of dry ethanol added to it. The solution reflected for 2 h in 40 °C. After sample was cold, solid material was filtered by Buchner funnel. The obtained sediment was washed with 30 mL of dry ethanol and then it was set in autoclave for 1 h in 40 °C. The certain amount of synthesized mesoporous silicate transferred into balloon having 0.1 g of titanium butoxide in 30 mL of dry alcohol. The mixture reflected with strong rotation for 2 h at 40 °C. Titanium mesoporous silicate was provided according to linking method, using titanium butoxide and mesoporous silicate with mole per cent  $\left(\frac{\text{Ti}}{\text{Ti} + \text{Si}} = 2\right)$ . Replacement reaction happened between superficial Si-OH groups inside cavities and butoxy titanium groups and connected Ti into cavities (Fig. 2).

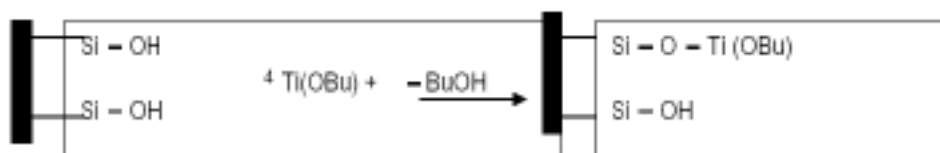


Fig. 2. A sight of replacement reaction between superficial Si-OH groups inside cavities with butoxy titanium groups

The sediment filtered by Buchner funnel and washed with dry alcohol several times. During night, it was set in autoclave at 40 °C. The sample was calcinated to remove butyl groups, connected to Ti and organic gross in a furnace with temperature setting. The temperature was increased from ambient temperature to 550 °C with 3 °C/min temperature slant and then the sample remained at this temperature for 4 h. Temperature decreased to ambient temperature in the same speed.

As titanium butoxide easily hydrolyzed with little water and dried alcohol used in this test. In addition, containers used for transferring this compound should be dry and should not be washed with water.

**Study of diffraction measurement of samples:** The strong peaks observed in X-ray diffraction measurement pattern of newly synthesized mesoporous before calcination as well as after calcinations. Comparing XRD spectrum with reference spectra for all kinds of mesoporous structure (Fig. 3), show similarity between obtained spectrum and the structure of spectrum related to MCM-41. MCM-41 has cavities with hexagonal structure. Comparing XRD spectra before and after calcinations shows that,  $d_{100}$  decreased from 36.68 Å related to XRD spectrum before calcinations to 36.04 Å. By placing this value in this formula ( $a = 2d_{100}/\sqrt{3}$ ), a, single parameter cell can be computed.  $a = 2d_{100}/\sqrt{3} = 42.36$  Å before calcinations  $a = 2d_{100}/\sqrt{3} = 41.62$  Å after calcinations.

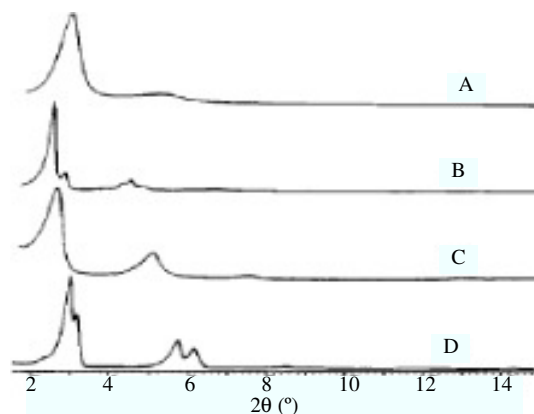


Fig. 3. XRD designs: (A) calcinated MCM-41 (B) calcinated MCM-48 (C) the structure of newly synthesized Lamar (D) cubic octahedron

The data related to calcinated materials has good conformity with whatever reported previously. Network compression due to calcinations can have more values according to synthesis conditions<sup>17</sup>.

Microprobe's examination indicate that changes in network size of these molecular sieves as a result of calcinations or drainage is very little. For example, the dimension of cubic unit (FAU)\* of newly synthesized cell is 24.565 Å and calcinated cell in 500 °C equals 24.519 Å<sup>18</sup>.

Comparing XRD spectrum of titanium mesoporous silicate with its pure silica spectrum indicates that mesoporous structure did not change after titanium adjunction and former structure was preserved (Fig. 4). The parameter of single cell was obtained ( $a = 42.85$  Å) by former formula. By adjoining Ti intermediate metal to meso structure,  $d_{100}$  peak of titanium mesoporous silicate was transferred to below angles and get wider. This indicated the expanding of network intervals as a result of titanium adjunction. Also, due to Ti adjunction, the parameter size of single cell increased to ZSM-5 structures<sup>19</sup>. Therefore, one of the cases, which confirm Ti connection into cavities of mesoporous silicate, is the transition of  $d_{100}$  peak in XRD pattern of this compound toward smaller angles. Fig. 5 shows the results of TGA newly synthesized mesoporous silicate. Thermal operation performed under argon atmosphere with 5 °C/min constant temperature slant up to 700 °C.

This sample shows three specific steps of weight reduction: 25-150 °C, 150-400 °C and more than 400 °C. The first step of weight reduction results is water re-absorption. The second step is indicative of the analysis of organic species (TMA, C<sub>16</sub>TMA). The third step is related to losing water as a result of condensation of silanol groups and formation of siloxan links. As shown in TGA chart, the sample includes 50 % of organic species weight. The results show that most organic moulds emitted by the analysis or re-absorption in neutral gas were below 400 °C.

\*Faujasite.

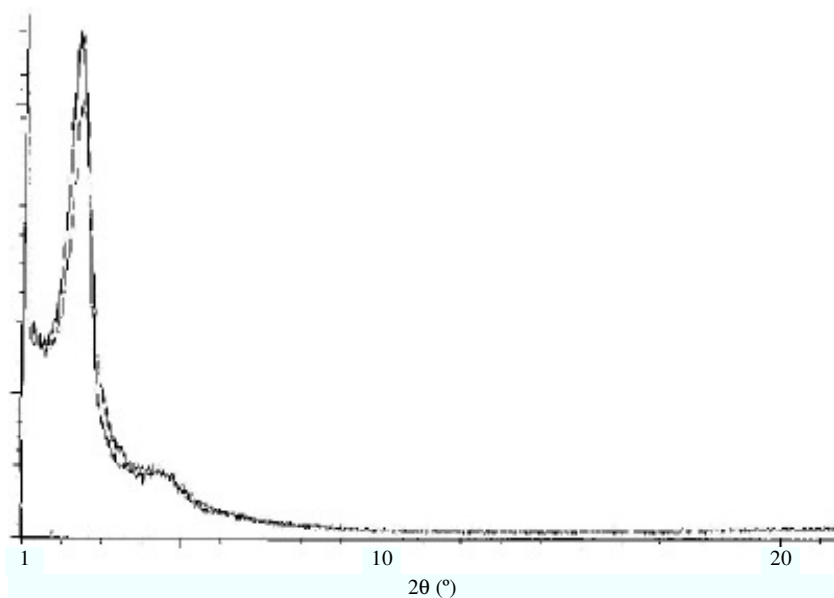


Fig. 4. Comparing the X-ray diffraction pattern of mesoporous silicate and its titanous compound

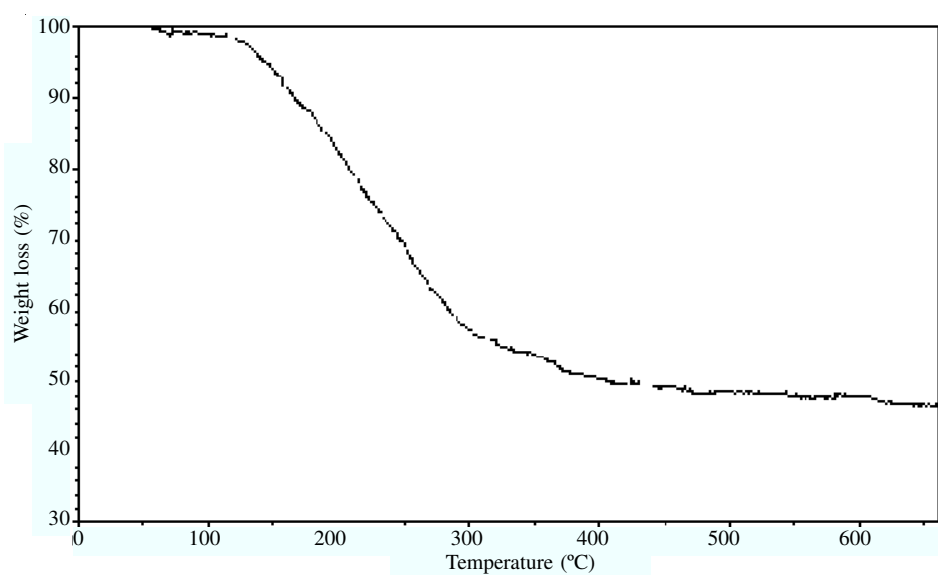


Fig. 5. TGA Design of newly synthesized mesoporous silicate

In this test for measuring microscopic spectrum, about 100 Å gold, which equals to 20 layers atom placed on sample. This layer is not thick enough to deorganize the structure. After conducting through putting gold on surface, the sample placed into the case of the device. Figs. 6 and 7 show particles of mesoporous silicate and

titanium mesoporous silicate, respectively. As it is obvious in the Figs. 6 and 7, the sample of pure silica has spherical particles with a range of 150-700 nm. In comparison with pure silica, it is observed that titanium mesoporous silicate has more condensed and smaller particles, about of 50-300 nm. In elemental analysis, the percentage of existent elements in the compound can be acquired in two elemental and oxide forms. Existing of gross in synthesized compound can be studied through elemental analysis. Fig. 8 is related to mesoporous silicate and Fig. 9 shows titanium mesoporous silicate. The results show that there is no gross in both materials. The per cent weight of  $\text{TiO}_2$  in proportion to total sample was 4.82 and the ratio of  $\text{SiO}_2$ - $\text{TiO}_2$  was about 20. Other observed peaks in the above figures were related to basis metal. The type of this metal was brass consisting of copper, zinc and gold which covers the compound (Fig. 10). It is worth mentioning that the values of these elements were not considered in former computations.

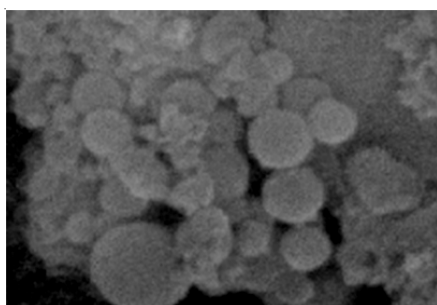


Fig. 6. SEM of mesoporous silicate in 500 nm scale

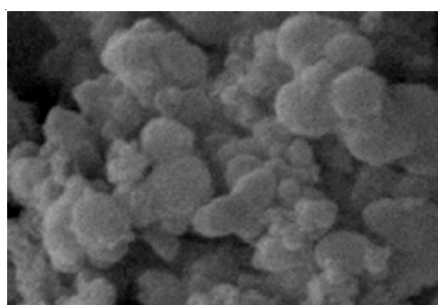


Fig. 7. SEM of titanium mesoporous silicate in 500 nm scale

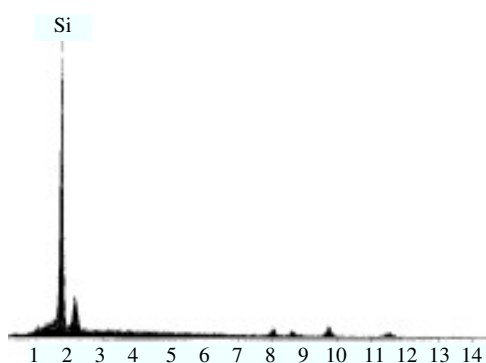


Fig. 8. Elemental analysis of mesoporous silicate

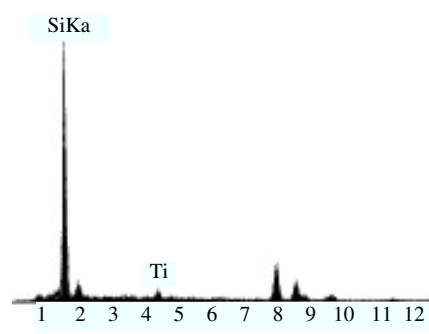


Fig. 9. Elemental analysis of titanium mesoporous silicate

IR spectrum of samples is usually used to determine titanium sites properties in molecular sieves of mesoporous<sup>12,20-22</sup>. Required pill provided using KBr for test performing. The Figs. 11 and 12 show the spectrum of mesoporous silicate and titanium mesoporous silicate, respectively. Comparing peaks positions with standard

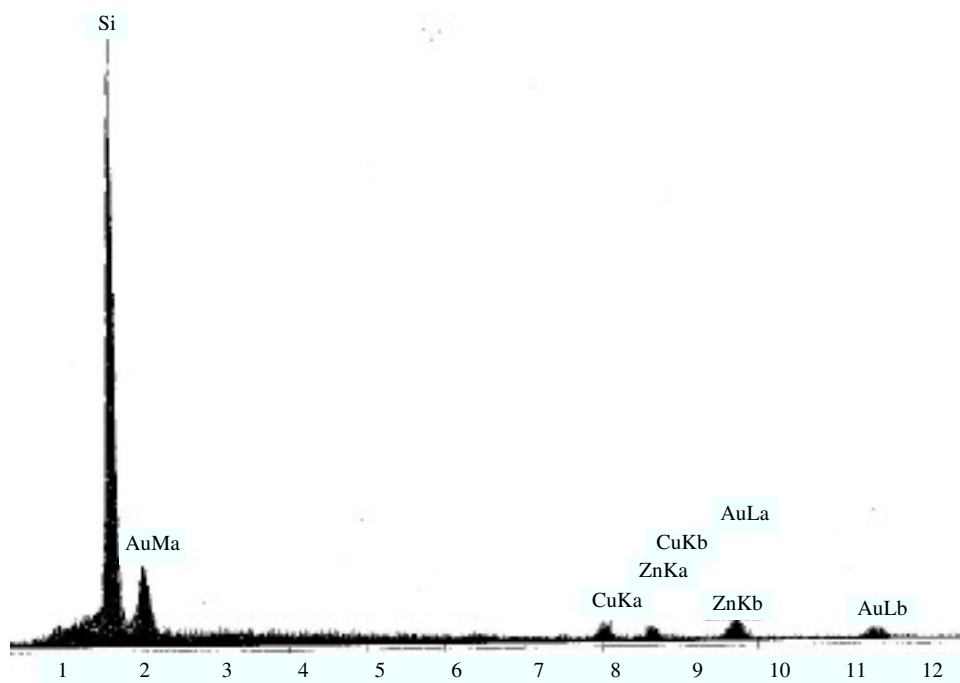


Fig. 10. Elemental analysis of mesoporous silicate in combination with basis and covering metals

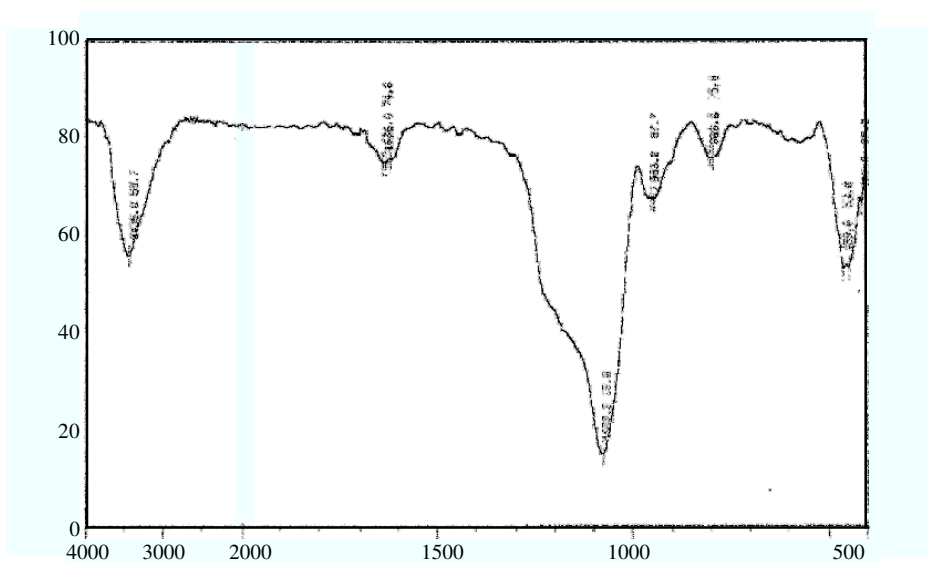


Fig. 11. IR spectrum of mesoporous silicate

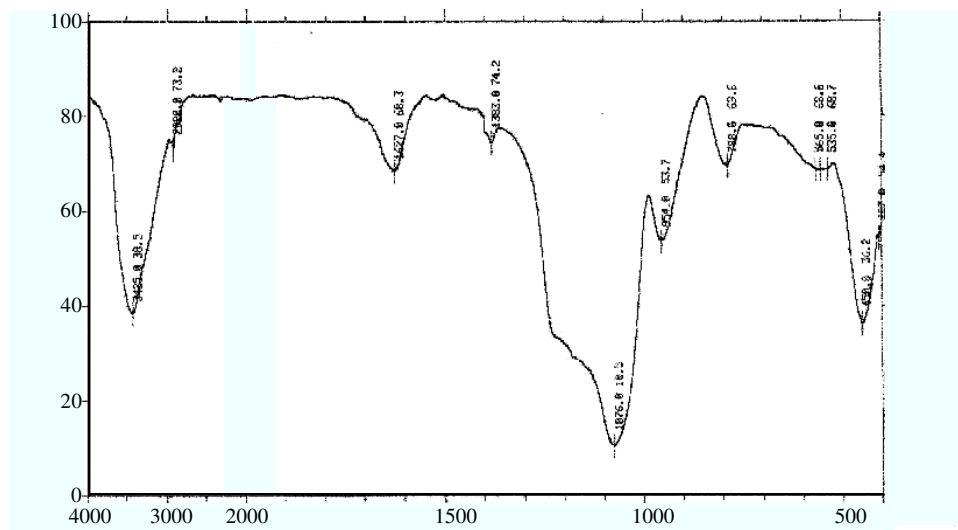


Fig. 12. IR spectrum of titanium mesoporous silicate

data, we can recognize factorial groups of these compounds. Referring to sources shows that strong peak in  $3700\text{--}3200\text{ cm}^{-1}$  areas is related to silanol groups (Si-OH) and its existence confirms silanol groups in the structure. It is notable that this compound has water and absorbs it in contact with environment. Therefore, the vibration of O-H group of water molecules with silanol group placed in one area. One of the characteristics of MCM-41 is existence of silanol groups<sup>23-27</sup>. A strong peak in a range of  $1100\text{--}1000\text{ cm}^{-1}$  is related to Si-O-Si, non-symmetric tensile vibration. With the participation of titanium atom in the frame of mesoporous silicate, a replacement about  $3\text{ cm}^{-1}$  was observed in these vibrations. Si-O-Si non-symmetric vibrations in mesoporous silicate and its titanous compound were almost  $1079$  and  $1076\text{ cm}^{-1}$ , respectively.

A vibration at *ca.*  $960\text{ cm}^{-1}$  was observed in IR spectrum of titanium mesoporous silicate. A similar band was found in zeolites spectrum having titanium such as TS-1, Ti- $\beta$ , Ti-ZSM-48 and other compounds. Three different interpretations have also been presented for this band. Boccuti *et al.*<sup>28</sup> ascribed this band to tensile mode of  $\text{SiO}_4$  units linked to titanium ion. Other researchers attributed this band to titanol groups<sup>29</sup> or Si-O tensile vibration in Si-O...H groups<sup>30</sup>. In sum, this band is also observed in non-titanium mesoporous as appeared  $953\text{ cm}^{-1}$  in spectrum of mesoporous silicate. But this band and  $800\text{ cm}^{-1}$  band resulting from  $\text{SiO}_4$ <sup>31</sup> symmetric tensile vibrations<sup>32</sup>, for titanous compounds is more than pure silica compounds. Therefore, it can be concluded that relative increase of  $960\text{ cm}^{-1}$  band is as a results of Ti adjunction to the structure<sup>33</sup>. Tables 1-3 indicates band positions and their factorial groups of every band. IR spectrum of mesoporous silicate and titanium mesoporous silicate has been compared in Tables 1-4.



TABLE-1  
BANDS POSITIONS AND RELATED FACTORIAL GROUPS

band position	Model	Structural unit
3200-3700	(OH) Tensional	Si-OH
3440	(OH) Tensional	H <sub>2</sub> O
1632	(H-O-H) bend	H <sub>2</sub> O
1000-1100	Asymmetric Si-O tensional	Si-O-Si
960	Asymmetric Si-O tensional	Si-O-H
800	Symmetric tensional Si-O	Si-O-Si
450-460	(O-Si-O) bend	O-Si-O

TABLE-2  
COMPARISON OF IR SPECTRUM OF MESOPOROUS SILICATE  
AND TITANIUM MESOPOROUS SILICATE

3700-3000 (cm <sup>-1</sup> )	3700-1000 (cm <sup>-1</sup> )	1000-400 (cm <sup>-1</sup> )	Sample
3430 Tensional Si-OH	1079 Asymmetric tensional Si-O-Si	953 Asymmetric Si-tensional OH	Mesoporous silicate
3425 tensional Si-OH	1076 Asymmetric tensional Si-O-Si	954 Asymmetric Si-tensional and O-Si, Si-O-Ti	Titanium mesoporous silicate

TABLE-3  
SUMMARY OF THE RESULTS RELATED TO CALCULATION OF  
THICKNESS OF CAVITIES WALLS

	2θ	d <sub>100</sub>	a	Cavity diameter	Wall thickness
MS	2.45	36.05	41.62	37.24	4.38
TMS	2.38	37.11	42.85	35.69	7.16

**Superficial absorption of nitrogen:** Most solids are porous and many techniques have been developed to examine their characteristics. Among these techniques, superficial absorption of nitrogen is one of the most well known techniques. Information about cavity volume [PV(cm<sup>3</sup> g<sup>-1</sup>)], BET superficial area [Sg(m<sup>2</sup> g<sup>-1</sup>)] and the distribution of cavities sizes is obtained from this technique.

TABLE-4  
COMPARISON OF QUANTITIES OF SUPERFICIAL ABSORPTION  
ANALYSIS OF NITROGEN IN TWO SAMPLES

Superficial area longmeyer (m <sup>2</sup> g <sup>-1</sup> )	Cavities diameter (Å) mean	Cavity volum (cm <sup>3</sup> g <sup>-1</sup> )	Superficial area BET (m <sup>2</sup> g <sup>-1</sup> )	Sample
1521	37.24	1.2435	1088	Mesoporous silicate
1501	35.69	1.2426	1076	Titanium mesoporous silicate

Absorption isotherm shows the relationship of the amount of absorbed material in the balance pressure of gas with constant temperature. Fig. 13 shows absorption, re-absorption isotherm of mesoporous silicate. Usually in these isotherms, re-absorption isotherms do not return to the same absorption path, but places a little upper than it. Fig. 14 indicates absorption and re-absorption isotherm after adjunction of titanous compound to the structure. As mentioned before, one of the obvious characteristics of these materials is high superficial area ( $> 1000 \text{ m}^2 \text{ g}^{-1}$ ). Fig. 15 shows BET chart of mesoporous silicate. Its superficial area was obtained at  $1088 \text{ m}^2 \text{ g}^{-1}$  using this information and related equations.

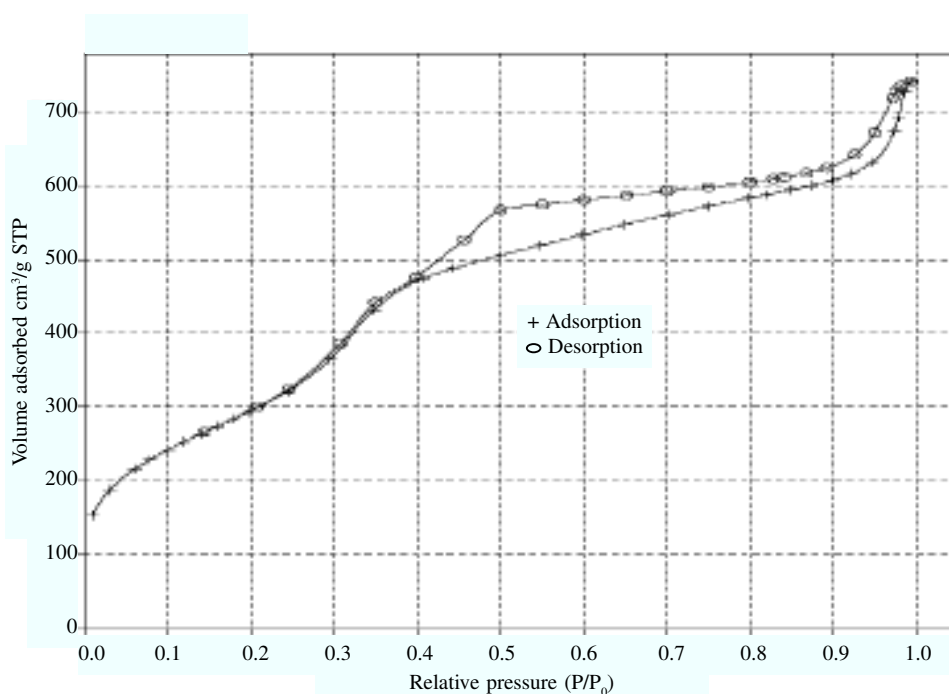


Fig. 13. Adsorption, re-adsorption isotherm of mesoporous silicate

Fig. 16 shows BET chart of titanium mesoporous silicate. BET value decreased to  $1076 \text{ m}^2 \text{ g}^{-1}$  in this compound. Another reason for linking titanium into structure is decreasing of cavities volumes because of titanium adjunction to their inside. BJH is a calculation method for measuring cavities volumes. Barret, Joyner and Hellenda (BJH) introduced this method for the first time, so it is well-known by this name. Studying and comparing cavities volumes before and after titanium adjunction indicates that cavity volume has decreased from  $1.2435\text{-}1.2426 \text{ cm}^3 \text{ g}^{-1}$ . Therefore, the decrease of superficial area and cavity volume after titanium adjunction show that titanium has chemically been linked into mesoporous cavities.

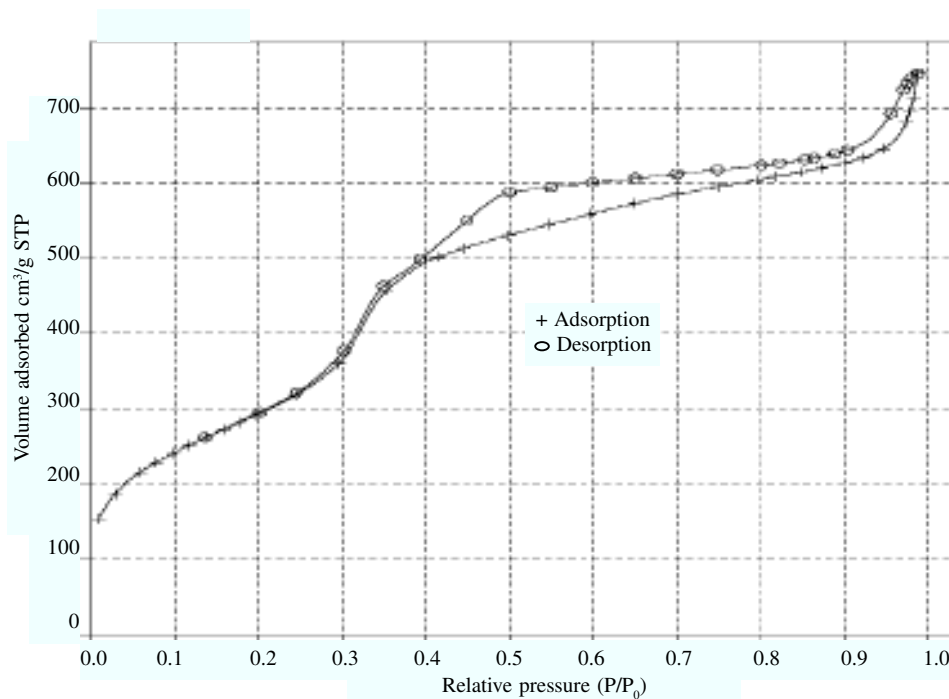


Fig. 14. Absorption, re-absorption isotherm of titanium mesoporous silicate

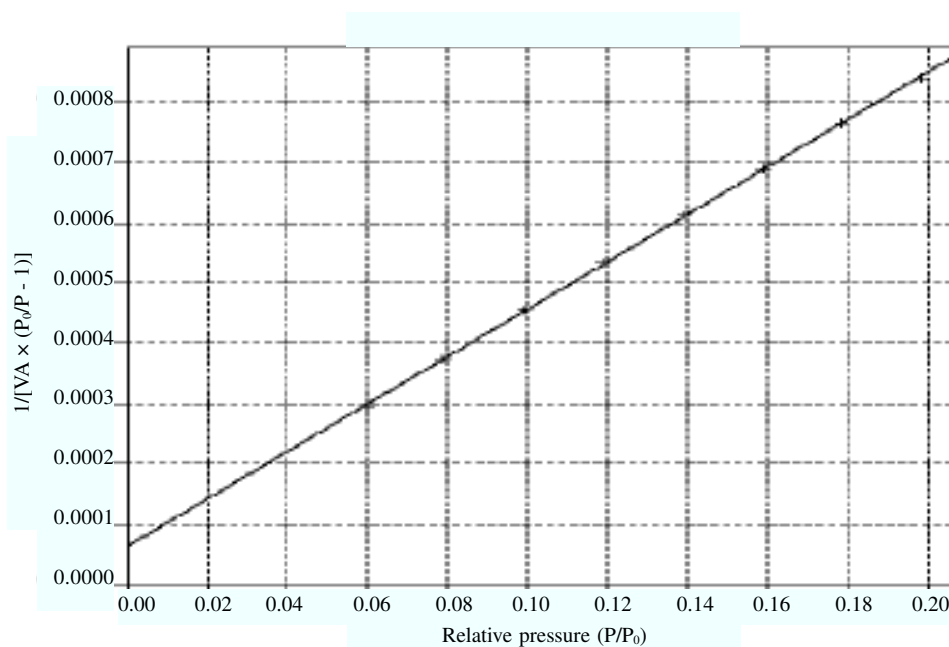


Fig. 15. BET Chart of mesoporous silicate

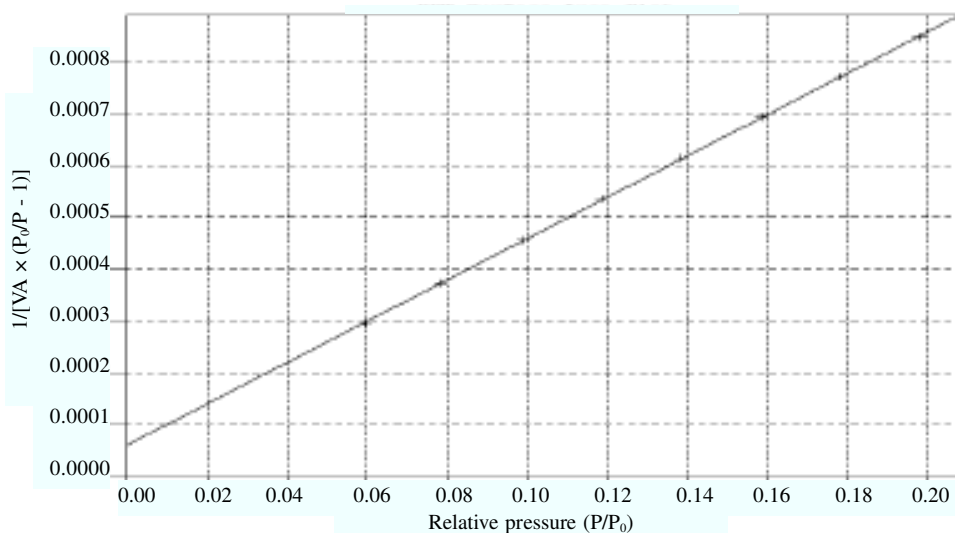


Fig. 16. BET Chart of titanium mesoporous silicate

Another characteristics of this group of mesoporous, which is distinguishing them from natural mesoporous is narrow distribution of cavities sizes in these materials. Fig. 17 shows distribution curve of BJH cavities sizes for mesoporous silicate. In this chart  $dA/d \log(D)$  quantity has been drawn according to cavities diameters. This curve maximum indicates isomorphic meso cavities with 3.72 nm approximate diameter. Fig. 18 shows distribution curve of BJH cavities sizes for titanium

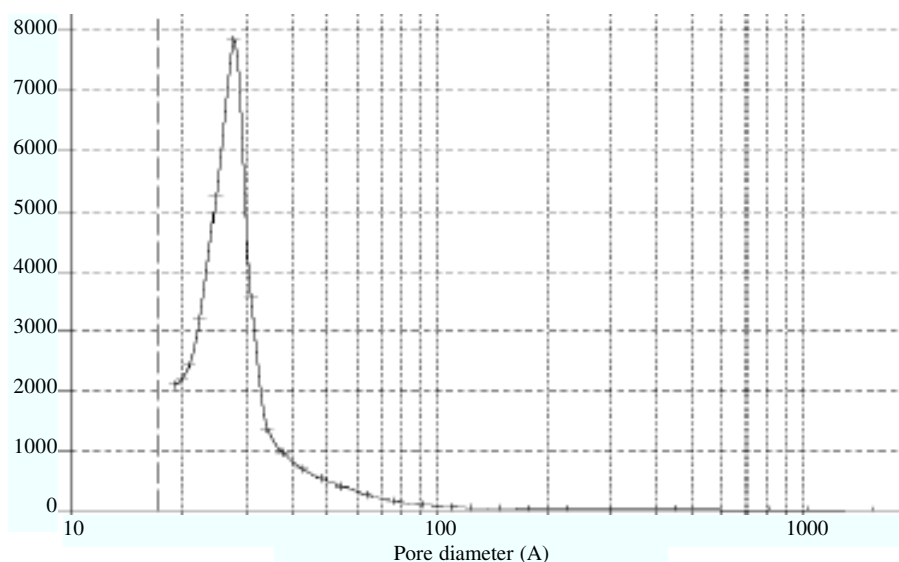


Fig. 17. Distribution curve of cavities sizes of mesoporous silicate

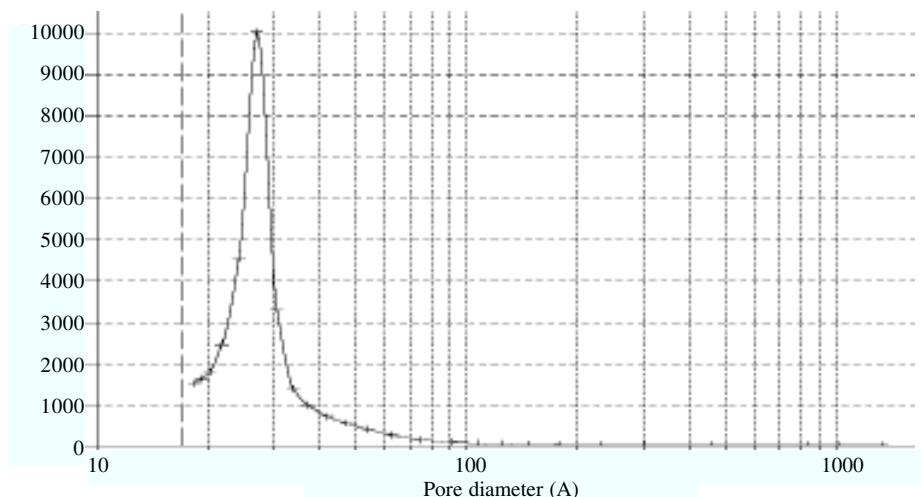


Fig. 18. Distribution curve of cavities sizes of titanium mesoporous silicate

mesoporous silicate. Comparing two curves indicates that the mean of cavities diameters decreased to 3.57 nm. This decreasing confirms titanium adjunction into cavities.

#### Computation of thickness of cavities walls

**Calculation of cavity wall thickness:** As mentioned in XRD part, from  $d_{100}$  position of this spectrum the single cell parameter which is the sum of cavity diameter and wall thickness can be computed by a  $a = 2d_{100}/\sqrt{3}$  formula. The mean of cavity diameter of mesoporous silicate obtained 37.24A used BJH method. Wall thickness(e) was obtained by subtracting a from the mean of cavity diameter.  $e = 41.62 - 37.24 = 4.38A$ . By performing these steps, titanium derivative equals to:  $e = 42.85 - 35.69 = 7.16A$ .

Increasing of wall thickness is another reason for titanium adjunction into cavities. The results are summarized in Tables 1-5. The results of superficial absorption analysis of nitrogen have been given in Table-4.

TABLE-5  
RESULTS OF XRF QUANTITATIVE ANALYSIS

Standard error	Weight (%)	Compound name
0.09	96.27	SiO <sub>2</sub>
0.09	3.48	TiO <sub>2</sub>
0.04	45.00	Si
0.05	2.09	Ti

Weight per cent in oxidal and elemental forms has been shown in Table-5 using X-ray (XRF). With regard to this analysis, TiO<sub>2</sub> weight per cent and elemental titanium were obtained 3.48 and 2.09, respectively. Gross per cent was very little (Table-6).

TABLE-6  
GROSS AMOUNT OF TITANIUM MESOPOROUS SILICATE

Standard error	Weight (%)	Compound name
0.0080	0.1080	Al <sub>2</sub> O <sub>3</sub>
0.0014	0.0287	Fe <sub>2</sub> O <sub>3</sub>
0.0017	0.0203	S
0.0015	0.0184	CaO
0.0023	0.0161	Cl

## RESULTS AND DISCUSSION

As mentioned before, after synthesis of mesoporous silicate and titanium mesoporous silicate, its characteristics and structure were studied. To recognize and examine the structure of synthesized compounds, diffraction technique of X-ray in low angles (LAXRD), infrared spectrometry (IR), thermal analysis (TGA), superficial absorption of nitrogen, scanning electronic microscope (SEM), elemental and oxidal analyses by SEM, quantitative analysis of X-ray fluorescence (XRF) had been used. For determining suitable temperature to calcinate newly synthesized mesoporous silicate and emitting organic mould, it is necessary to specify the temperature in which the mould exited completely by studying TGA analysis. The results of TGA analysis showed that organic mould exits completely to 400 °C. It is also obvious that collapse in the structure has not been obtained up to 700 °C. Therefore, the temperature more than 400 °C and less than 700 °C is a suitable one to calcinate 550 °C with 3 °C/min temperature slant which was selected. Measuring diffraction of existent X-ray does not specify 2θs less than 8. So, the spectra of two compounds from 1-30 recorded 2θ using diffraction measuring of X-ray with ability to analysis in low angles. The 2θ values more than 10 were recorded for studying the presence or lack of presence of amorphous silica or other undesirable peaks. As expected, any peak indicative of such compounds was not observed. Hexagonal structure of cavities was proved using the information of XRD and its comparison with former synthesized compound of this group. The size of single cell parameter belonged to XRD spectrum was computed and for newly synthesized, calcinated and titanous mesoporous silicate obtained 42.36, 41.62 and 42.85, respectively. The decrease in single cell parameter as a result of calcinations is because of network compression.  $d_{100}$  transition to smaller angles and the increase of single cell parameter to 42.85 Å is a reason for Ti adjunction to the structure. Cavities diameters with the use of superficial absorption of nitrogen obtained 37.24 and 35.69, respectively that was mesoporous range. The difference of single cell parameter with diameter of cavities obtained from superficial absorption of nitrogen resulted in 4.38 and 7.16 Å wall thickness for mesoporous silicate and titanium mesoporous silicate. Increasing thickness is another reason for Ti adjunction to the structure. High superficial area of these compounds is considered their evident characteristics, which were 1088 and 1076 m<sup>2</sup>/g, respectively.

Narrow distribution of cavities sizes shows isomorphic meso cavities in the compound. While in other natural compounds, the large area of cavities sizes and wide arched chart were observed. Comparing BET values with former reported values shows that synthesized compound has good superficial area. Deflation electronic microscope or SEM determines compounds morphology that comparing obtained SEMs with reference SEM confirms spherical morphology of the structure. Also, using this technique determines the existing of gross in compound and weight per cent of compounds in two oxidal and elemental forms. The results showed that there is no considerable gross and the weight of titanium oxide was 4.82 %. The results of this analysis did not possess high accuracy, so XRF analysis performed quantitatively. XRF analysis reported quantitative gross in the compound and also the amount of titanium of structure and weight per cent of oxide titanium were reported 2.09 and 3.48, respectively.

TGA and IR techniques determine that the mould is completely exited. The results of IR spectrometry had good conformity with reported spectra in authorities. Factorial groups of mesoporous such as (Si-OH) synalol and Si-O-Si, symmetric and non-symmetric tensile vibrations and also deflections are obvious in this spectrum. IR spectrum of titanium mesoporous silicate was also studied. The results showed that peaks replacement and intensity increase, which in particular cases related to Ti linking, confirms Ti adjunction to the structure.

## REFERENCES

1. X.S. Zhao, G.Q. Lu and G.J. Millar, *Ind. Eng. Chem. Res.*, **35**, 2075 (1996).
2. G. Centi and M. Misono, *Catal. Today*, **41**, 287 (1998).
3. R.A. Sheldon, I.W.C.E. Arends and H.E.B. Lempers, *Catal. Today*, **41**, 387 (1998).
4. M. Taramasso, G. Perego and B. Notari (SNAM Progetti S.P.A.) U.S.P. 4410501 (1983); *Chem. Abstr.*, **95**, 206272k (1981).
5. B. Notari, *Catal. Today*, **18**, 163 (1993).
6. A. Corma, M.A. Cambor, P. Esteve, A. Martinez and J. Perez-Pariente, *J. Catal.*, **145**, 151 (1994).
7. D.P. Serrano, H.X. Li and M.E. Davis, *J. Chem. Soc. Chem. Commun.*, 745 (1992).
8. M.A. Cambor, A. Corma, A. Martinez and J. Perez-Pariente, *J. Chem. Soc. Chem. Commun.*, 589 (1992).
9. N. Ulagappan and V. Krishnasamy, *J. Chem. Soc. Chem. Commun.*, 373 (1995).
10. M.H. Zahedi-Niaki, P. Narahar and S. Kaliaguine, *Chem. Commun.*, 47 (1996).
11. L. Marchese, A. Frache, S. Coluccia and J.M. Thomas, Proceedings of the 12th International Zeolite Conference (Eds.: M.M.J. Treacy, B.K. Marcus, M.E. Bisher and J.B. Higgins), Materials Research Society, Warrendale, Pennsylvania, pp. 1569-1576 (1998).
12. C.T. Kresge, M.E. Leonowicz, W.J. Roth, J.C. Vartuli and J.S. Beck, *Nature*, **359**, 710 (1992).
13. A. Corma, M.T. Navarro and J. Pe rez-Pariente, *J. Chem. Soc. Chem. Commun.*, 147 (1994).
14. W. Zhang, M. Fr ba, J. Wang, P.T. Tanev, J. Wong and T.J. Pinnavaia, *J. Am. Chem. Soc.*, **118**, 9164 (1996).
15. P.T. Tanev, M. Chibwe and T.J. Pinnavaia, *Nature*, **368**, 321 (1994).
16. M. Morey, A. Davidson and G. Stucky, *Microporous Mater.*, **6**, 99 (1996).
17. A. Corma, J.L. Jorda, M.T. Navarro and F. Rey, *Chem. Commun.*, 1899 (1998).
18. C.-Y. Chen, S.L. Burkett, H.-X. Li and M.E. Davis, *Microporous Mater.*, **2**, 27 (1993).

19. U. Henriksson, L. Odberg, J.C. Eriksson and L. Westman, *J. Phys. Chem.*, **81**, 76 (1977).
20. H. Van Koningsveld, J.C. Jansen and H. Van Bekkum, *Zeolite*, **10**, 235 (1990).
21. J.S. Reddy, A. Dicko and A. Sayari, In *Synthesis of Microporous Materials: Zeolites, Clays and Nanostructures*; Eds.: M.L. Occelli and H. Kessler, Marcel Dekker: New York, in press.
22. A. Corma, M.T. Navarro, J. Perez-Pariente and F. Sanchez, *Stud. Surf. Sci. Catal.*, **84**, 69 (1994).
23. A. Sayari, V.R. Karra, J.S. Reddy and I.L. Moudrakovski, *Mater. Res. Soc. Symp. Proc.*, **371**, 81 (1995).
24. G. Perego, G. Bellussi, C. Corno, M. Taramasso, F. Buonomo and A. Esposito, *Stud. Surf. Sci. Catal.*, **28**, 129 (1986).
25. J.L. Blin, A. Leonard and B.L. Su, *Chem. Mater.*, **13**, 3542 (2001); G. Herrier, J.L. Blin and B.L. Su, *Langmuir*, **17**, 4422 (2001).
26. K.M. Reddy, I.L. Moudrakovski and A. Sayari, *J. Chem. Soc. Chem. Commun.*, 1491 and references therein (1994).
27. K.M. Reddy, S. Kaliaguine and A. Sayari, *Catal. Lett.*, **23**, 169 (1994).
28. K.M. Reddy, S. Kaliaguine, A. Sayari, A.V. Ramaswamy, V.S. Reddy and L. Bonneviot, *Catal. Lett.*, **23**, 175 (1994).
29. M. Boccuti, K.M. Rao, A. Zecchina, G. Leofanti and G. Petrini, *Stud. Surf. Sci. Catal.*, **48**, 133 (1989).
30. D.R.C. Huybrechts, I. Vaesen, H.X. Li and P.A. Jacobs, *Catal. Lett.*, **8**, 237 (1991).
31. M.A. Camblor, A. Corma and J. Perez-Pariente, *J. Chem. Soc. Chem. Commun.*, 557 (1993).
32. R. Szostak, *Molecular Sieves: Principles of Synthesis and Identification*; Van Nostrand: New York, p. 316 (1989).
33. V.N. Rajakovic, S. Mintova, J. Senker and T. Bein, *Mater. Sci. Eng.*, **23**, 817 (2003).